Comparative Research on Laminar Flame Propagation for Four C8 Fuels

Xin Meng *, Shuai Liu, Jing Tian, Ruina Li, Tao Sun

Posted Date: 1 October 2024

doi: 10.20944/preprints202409.2458.v1

Keywords: Laminar flame speed Butyl ether; N-octane; Iso-octane; 1-octene; Chemical kinetics

 doi:10.20944/preprints202409.2458.v1

Article

Comparative Research on Laminar Flame Propagation for Four C_8 Fuels

Xin Meng [1,*], Shuai Liu [2], Jing Tian [1], Ruina Li[2] and Tao Sun [1]

[1] School of Mechanical and Electrical Engineering, Xuzhou University of Technology, Lishui Road 2, Xuzhou 221018, China
[2] School of Automotive and Traffic Engineering, Jiangsu University, Xuefu Road 301, Zhenjiang 212013, China
* Correspondence: mengxin@xzit.edu.cn

Abstract: Experimental studies and numerical analyses were conducted to estimate the laminar flame speeds of butyl ether, n-octane, iso-octane, and 1-octene at temperatures of 373 and 443 K and pressures ranging from 0.03 to 0.3 MPa in a constant-volume combustion chamber. Iso-octane had the slowest laminar flame speed whereas butyl ether had the highest. The LLNL model for large hydrocarbons and the Cai model for butyl ether were combined to describe the chemical kinetic mechanism for the test fuels. The simulation data calculated with the constructed model agree with the experimental data. The discrepancies in the laminar flame speeds of the four fuels were clarified from the perspectives of thermodynamics, diffusion, and chemical kinetics. The results reveal that the thermodynamics and chemical kinetics were dominant. Butyl ether had the highest laminar flame speed. This was attributed to it having the highest adiabatic flame temperature and a higher concentration of H and OH radicals, which have a high reactivity in a flame. Iso-octane produces the highest concentration of CH_3, which inhibits flame propagation, so that it had the slowest laminar flame speed.

Keywords: laminar flame speed; butyl ether; N-octane; Iso-octane; 1-octene; chemical kinetics

1. Introduction

Petroleum fuel will still be the main energy source for transportation for a long time. However, air pollution caused by fossil fuels and energy crises have become global problems. Thus, efficient clean combustion technologies are being developed for petroleum fuels. Furthermore, clean renewable fuels can replace traditional fossil fuels. An in-depth understanding of the combustion characteristics of fuels is a prerequisite for clean combustion. Petroleum fuels have thousands of components, mainly alkenes, aromatics, alkanes, branched alkanes, and cycloalkanes. Therefore, it is necessary to investigate the combustion characteristics of alternative fuels and the representative components of fossil fuels.

In this research, iso-octane, which has a low reactivity, was used as typical representative of fuels that are difficult to self-ignite. As an isomer of iso-octane, n-octane, which has an octane rating of −10, was selected as the representative of fuels with self-ignition characteristics. 1-octene, which has a similar structure to n-octane, represented macromolecular olefins. Butyl ether, which has a straight chain, was chosen to be the representative macromolecule oxygenated alternative fuel. Table 1 lists the properties and structure of the four test fuels.

The laminar flame speed is commonly used to confirm the chemical mechanism and is also useful when designing a combustor. Laminar flame propagation was comparatively studied in this paper for the four C8 fuels. Iso-octane is an alternative to gasoline, so its combustion characteristics have been extensively researched. The laminar flame speed of iso-octane was obtained at atmospheric pressure and 353 K under several experimental setups by Kelly et al.[1]. Ji et al.[2] (2012) studied the laminar flame speed of iso-octane for the same condition as Kelly using the counterflow flame

 doi:10.20944/preprints202409.2458.v1

method. The laminar flame speed of iso-octane was measured over a wider range of experimental conditions by Galmiche et al[3] (T = 323 – 473 K and P = 0.1 – 1.0 MPa) and Broustail et al[4] (T = 423 K and P = 0.1 – 1.0 MPa) using outwardly propagating spherical flames. The laminar flame speeds of iso-octane at high pressure are available, but no data for low pressures have been reported.

Table 1. The properties and structure of the four test fuels.

	iso-octane	*n*-octane	1-octene	Butyl ether
molecular formula	C_8H_{18}	C_8H_{18}	C_8H_{16}	$C_8H_{18}O$
molecular structure	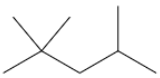	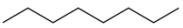	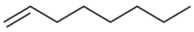	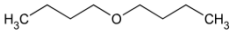
oxygen content/%	0	0	0	12.3
boiling point/K	372.3	398.5	395	414
low heat value/MJ·kg^{-1}	44.4	44.5	-	38

There are few works in the literature on the combustion characteristics of n-octane. Kelly et al.[5] studied the laminar flame speed of n-octane at an initial temperature of 353 K and pressures ranging from 0.1 to 0.5 MPa. Ji et al.[6] investigated the laminar flame speeds of n-octane at 353 K and atmospheric pressure. Thus, the laminar flame speed of n-octane needs to be measured over a wider range of experimental conditions.

Meng et al[7] obtained the concentrations of intermediate species of 1-octene using a jet-stirred reactor (JSR). The emission characteristics of 1-octene were measured for a single-cylinder engine by Hellier et al.[8]. There are no reports in the literature on the laminar flame speed of 1-octene.

Research into the combustion characteristics of butyl ether have focused on its chemical kinetics. Cai et al.[9] measured the concentrations of intermediate species of butyl ether and its laminar flame speeds with a JSR at a temperature of 373 K and a pressure of 0.1 MPa. The combustion mechanism of butyl ether was proposed based on the experimental data. Guan et al.[10] used a shock tube to measure the ignition delay time of butyl ether for temperatures ranging from 1100 to 1570 K and pressures ranging from 1.2 to 4 atm. Wullenkord et al.[11] investigated the structure and concentrations of intermediate species in the flame of butyl ether at a low pressure of 4 kPa. Thus, further experimental data on the combustion characteristics of butyl ether over a wider range of experimental conditions is needed.

This work is a comparative study of the laminar flame speeds of butyl ether, n-octane, iso-octane, and 1-octene. The first objective is to obtain the laminar flame speeds of the four test fuels over a wide range of experimental conditions. These speeds are then compared, and the differences are analyzed from the perspectives of thermodynamics, diffusion, and chemical reaction kinetics.

2. Experimental Setup and Data Post-Processing

2.1. Experimental Setup

Outwardly propagating spherical flames were used to obtain the laminar flame speed in this study. The constant-volume combustion bomb was cylindrical, 5.58 L in volume, and made of

 doi:10.20944/preprints202409.2458.v1

stainless steel. Two round pieces of quartz glass with diameters of 100 mm and a thickness of 60 mm were mounted opposite each along the same optical path. The test mixtures were prepared in a stainless mixing tank with a volume of 20 L. Fuel, oxygen, and nitrogen were sequentially injected into the mixing tank, and their partial pressures were determined by Dalton's law of partial pressure. Electronic heating tape, which can be heated up to 473 K, was wrapped around the combustion chamber and mixing tank. The temperature inside the chamber and mixing tank was measured with K-type thermocouples. A PID controller (CNil16, Omega) with an accuracy of 3 K was used to maintain the temperature inside the combustion chamber and mixing tank at the target level. Two pressure transmitters (3051, Rosemount) were mounted on the chamber and mixing tank to measure the steady pressure inside. A pressure transducer (7001, Kistler) was used to capture the explosive pressure in the combustion chamber. To ensure they were adequately mixed, the experimental mixtures were left in the mixing tank for at least 1 h before being introduced into the combustion chamber. The mixtures in the combustion chamber were ignited by a pair of electrodes mounted in the center of the chamber. A high-speed digital camera (V611, Phantom) with a sampling frequency of 10,000 frames per second was used to record the whole process of flame propagation. The image recording system, pressure measuring system, and ignition system were synchronized by a digital pulse generator (DG535). The image and pressure acquisition signals were sent at the same time, and the ignition signal was sent after a 1 ms delay. Each test was repeated three times to increase the accuracy of the experimental data.

The purities of iso-octane, n-octene, n-octane, and butyl ether (Aladin) used in this study were all above 99.5%. To investigate the effects of pressure and temperature on the laminar flame speeds, experiments were performed at different initial pressures (0.03, 0.05, 0.1, 0.2, or 0.3 MPa) with a fixed temperature of 373 K, and different initial temperatures (373 or 443 K) at 0.1 MPa. Because of spontaneous ignition at 443 K, the highest measured temperature for butyl ether was 433 K rather than 443 K at atmospheric pressure. To verify the credibility of this experiment, the laminar flame speed of iso-octane was additionally measured at 423 K and 0.1 MPa. Table 2 lists the experimental conditions used in this study.

Table 2. Experimental conditions of laminar flame speed .

Fuel	T_u/K	P_u/MPa	ϕ
n-octane	373, 443	0.03–0.3	0.7–1.5
Iso-octane	373, 423, 443	0.03–0.3	0.7–1.5
1-octene	373, 443	0.03–0.3	0.7–1.5
Butyl ether	373, 433	0.03–0.3	0.7–1.5

2.2. Range of Values for the Spherical Flame Radius

Based on various factors, the outward propagation of a spherical flame can be divided into three stages[12]. The first stage starts at ignition and the formation of the flame core to the stable propagation of the flame. In this process, as the flame develops, the influence of the ignition energy on flame propagation gradually weakens and eventually ceases[12,13]. The second stage is the quasi-steady propagation stage. The effect of the ignition energy has ceased, while the effect of containment by the chamber begins to influence flame propagation. In this stage, the stretching rate dominates flame propagation. Therefore, the experimental data in this stage are post-processed. In the third stage, the containment by the combustion chamber results in gradually slower flame propagation [14].

As mentioned above, it is necessary to find the range of values for the spherical flame radius during the quasi-steady segment. Considering the size of the constant-volume bomb used in this

 doi:10.20944/preprints202409.2458.v1

study and our previous experience, the range 10–22 mm was applied in the post-processing in this paper. This range changes for different fuels and experimental conditions. At equivalence ratios close to stoichiometric ratios, the range has to be increased appropriately, which is done by reducing the lower limit to 7–8 mm. However, the initial radius should be increased appropriately for lean and rich equivalence ratios. To guarantee ignition at low pressures, the ignition energy is higher, resulting in a greater influence on flame propagation. Hence, at low pressures, the range used for post-processing was from 14 to 26 mm in this paper. Additionally, flame images with cellular structures were eliminated before the data were post-processed.

2.3. Extrapolating the Laminar Flame Speed

The data from the quasi-steady propagation stage need to be further post-processed to eliminate the effect of the stretch ratio during flame propagation. This post-processing results in an unstretched flame speed, S_b^0. In this paper, linear and nonlinear extrapolation methods were compared.

The linear extrapolation approach was proposed by Wu and Law[15]:

$$S_b^0 = S_b - L_b k \tag{1}$$

where L_b is the Markstein length, S_b is the propagation speed of a stretched flame, and k is the stretching rate. The propagation speed of a stretched flame is calculated by differentiating the spherical flame radius with respect to time:

$$S_b = \frac{dr}{dt} \tag{2}$$

The stretching rate is defined as:

$$k = \frac{1}{A}\frac{dA}{dt} = \frac{2S_b}{r} \tag{3}$$

However, under most conditions, the flame propagation speed has a nonlinear relation with the stretching rate. Therefore, nonlinear extrapolation methods are increasingly used. Currently, the most widely used nonlinear post-processing approach was developed by Kelly[12]:

$$\left(\frac{S_b}{S_b^0}\right)^2 \ln\left(\frac{S_b}{S_b^0}\right)^2 = -2\frac{L_b k}{S_b^0} \tag{4}$$

Finally, the laminar flame speed, S_u^0, can be obtained as follows:

$$S_u^0 = S_b^0 \rho_b / \rho_u \tag{5}$$

Where ρ_u and ρ_b are the unburned and burned gas densities, respectively.

2.4. Experimental Uncertainty Analysis

As well as the chamber confinement, ignition energy, flame instability, and extrapolation method, the measurement of the laminar flame speed is also impacted by buoyancy [16] and radiation[17,18]. To eliminate the influence of buoyancy, images with a flame floating up were removed during data post-processing. The radiation effect can be assessed using the Yu method[18], as follows:

$$S_{u,RCFS}^0 = S_{u,Exp}^0 + 0.82 S_{u,Exp}^0 (S_{u,Exp}^0 / S_0)^{-1.14} (T_u/T_0)(P_u/P_0)^{-0.3} \tag{6}$$

where T_0= 298 K, P_0= 0.1 MPa, and S_0 = 0.01 m·s^{-1}. $S_{u,RCFS}^0$ is the radiation-corrected laminar flame speed, and $S_{u,Exp}^0$ is the measured laminar flame speed.

The uncertainty of the laminar flame speed can be calculated by the method proposed by Moffat[19]:

$$\delta_{S_u^0} = \sqrt{(B_{S_L})^2 + \left(\frac{t_{M-1.95} S_{S_L}}{\sqrt{M}}\right)^2} \tag{7}$$

 doi:10.20944/preprints202409.2458.v1

where $t_{M-1.95}$ is the value from Student's t-distribution at the confidence interval of 95%, M is the number of times each experiment was repeated, S_{S_L} is the standard deviation of the propagation speed of an unstretched flame, and B_{S_L} is the total uncertainty for the outwardly propagating spherical flame, which is calculated as follows:

$$B_{S_L} = \sqrt{\sum_{i=1}^{n}\left(\frac{\partial S_L(x_i)}{\partial x_i}u_i\right)^2} \quad (8)$$

where x_i is the value of the ith factor and u_i is the uncertainty for the factor.

The laminar flame speed can be derived from the equivalence ratio (ϕ), the initial pressure, and the initial temperature, as follows:

$$S_u^0 = S_u^0(\phi)(T_u/T_{u0})^{\alpha_T(\phi)}(P_u/P_{u0})^{\beta_P(\phi)} \quad (9)$$

where the reference initial temperature T_{u0}=373 K and the reference initial pressure P_{u0}= 0.1 MPa.

The relative error for temperature was estimated to be under 1.5% since the accuracy of the thermocouple was ±3 K and the initial temperatures were 373 K and 443 K. The deviation of the actual pressure from the target pressure was controlled to be under ±1 kPa during the experiment, leading to a relative error for the pressure of within 1%. When preparing the mixtures, the liquid fuel was directly injected into the vacuum mixing tank, and the amount was calculated from the partial pressure measured by the static pressure transmitter. Then, N_2 and O_2 gas were introduced into the mixing tank. Therefore, the relative error of the equivalence ratio depends on the accuracy of the partial pressures of the fuel, O_2, and N_2, as measured by the pressure transmitter. Since the precision of the pressure transmitter was 0.075%, the relative uncertainty of the equivalence ratio was under 3%. It can be concluded that the total uncertainty for the laminar flame speed estimated in this research was within 1–4 $m \cdot s^{-1}$.

3. Numerical Method

The PREMIX codes in the CHEMKIN[20,21] software were used for the numerical calculations in this paper. The setup was consistent with the experimental conditions. To ensure the results had a high accuracy, the gradient parameters and solution curvature were set to 0.02, resulting in the calculation of up to 750 points.

The kinetic mechanism applied in this study is a combination of the C7–C20 large hydrocarbon model developed by the LLNL/NUI research group [22,23] and the butyl ether model proposed by Cai et al[9]. The LLNL mechanism was based on the NUI C0–C4 core mechanism, which is for linear and branched saturated alkanes, alkenes, and aromatics. The Cai mechanism for the low-temperature and high-temperature kinetics of butyl ether is based on the mechanism for n-butanol developed by Yasunaga et al.[24] from the NUI research group. Experimental data that included the ignition delay time, concentration of the species measured in the JSR, and the laminar flame speed were employed in this research to validate both mechanisms. The sub-mechanisms of aromatics, the C8 alkanes studied in this paper, and olefins were removed from the LLNL model resulting in a reduced mechanism that contains sub-mechanisms for 1-octene, n-octane, and iso-octane. Then, the sub-mechanism of butyl ether developed by Cai et al.[9] was coupled with the reduced mechanism.

4.Results and Discussion

4.1. Extrapolation of Laminar Flame Speeds

It is necessary to select the best post-processing method to ensure the accuracy of the experimental data. Both the linear and nonlinear extrapolation methods mentioned in Section 2.3 were adopted for data post-processing, and the results are given in Figure 1. The performance of the data post-processing methods depends on the Lewis number (*Le*)[25,26]. As Figure 1(a) shows, the propagation speed of a stretched flame had a linear relation with the stretching rate when *Le* was

 doi:10.20944/preprints202409.2458.v1

close to 1. The results obtained by the nonlinear extrapolation method are essentially the same as those calculated through the linear method. However, as Figure 1(b) shows, the relation between the stretching rate and stretched flame speed was nonlinear when *Le* deviated from 1. The linear extrapolation method overestimated the propagation speed of an unstretched flame. Obviously, the nonlinear extrapolation method performed better over a wider range of conditions. Therefore, the nonlinear extrapolation method was used for subsequent data post-processing in this study.

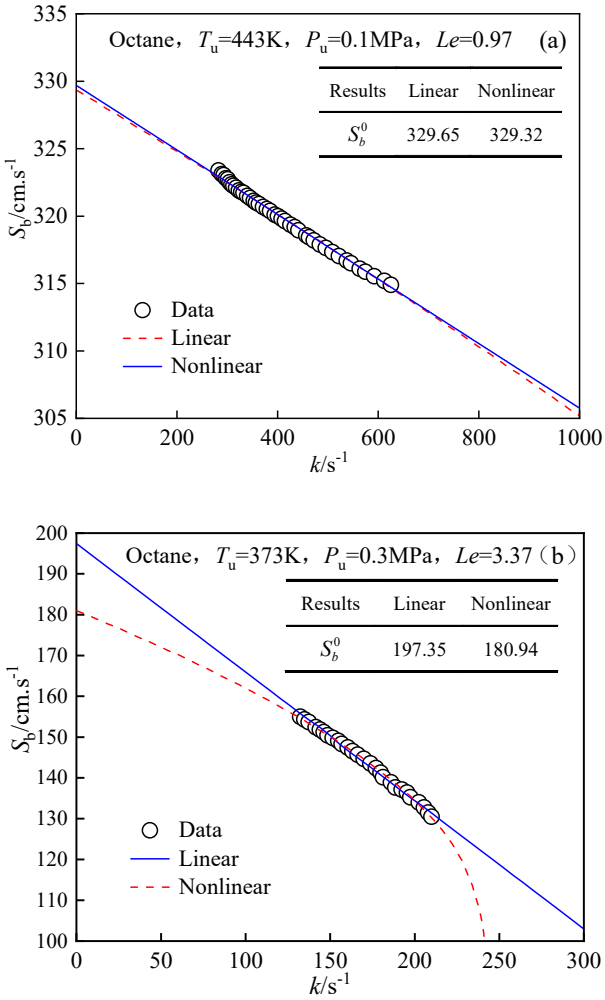

Figure 1. Comparison on unstretched flame speeds for n-octane extracted by nonlinear and linear methods at conditions: (a) $Le = 0.97$ and (b) $Le = 3.37$.

4.2. Validation of Experimental Setup

 doi:10.20944/preprints202409.2458.v1

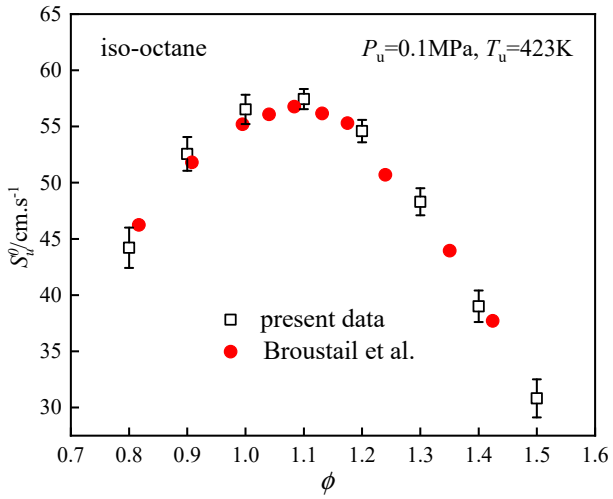

Figure 2. Comparison on laminar flame speeds of n-octane between the present experiment and the data measured by Broustail et al.

To verify the present experiment, the laminar flame speeds of iso-octane measured by Broustail et al.[4] were compared to the present experimental data obtained under the same conditions (T = 423 K and P = 0.1 MPa). The experimental method and data post-processing method were the same as those adopted in the experiment performed by Broustail et al. As shown in Figure 2, the present experimental data were slightly higher than those obtained by Broustail et al. near the stoichiometric ratio. The largest discrepancy was approximately 2.5 m·s^{-1} within the experimental uncertainty. There was good agreement at rich and lean equivalence ratios. Therefore, these results demonstrate that the present experimental data are credible. Because of a lack of experimental data in the literature, the laminar flame speeds for n-octane, 1-octene, and butyl ether could not be verified.

4.3. Laminar Flame Speeds Of n-Octane, Iso-Octane, 1-Octene, and Butyl Ether

Figure 3 shows the effect of pressure on the laminar flame speeds of the four test fuels. The initial pressure was inversely proportional to the laminar flame speed, so there was an increase in the laminar flame speed with a decrease in pressure. The relation between laminar flame speed and experimental conditions can be described as follows:

$$S_u^0 \sim P^{(n/2-1)} e^{-E_a/2R_0T_{ad}} \quad (10)$$

where n is the overall chemical reaction order, E_a is the overall activation energy, T_{ad} is the adiabatic flame temperature, and R_0 is the universal gas constant. The overall reaction order is usually between 1 and 2, so that the exponent for the pressure is negative, indicating that the laminar flame speed significantly increases with a decrease of the pressure, according to Eq. (10).

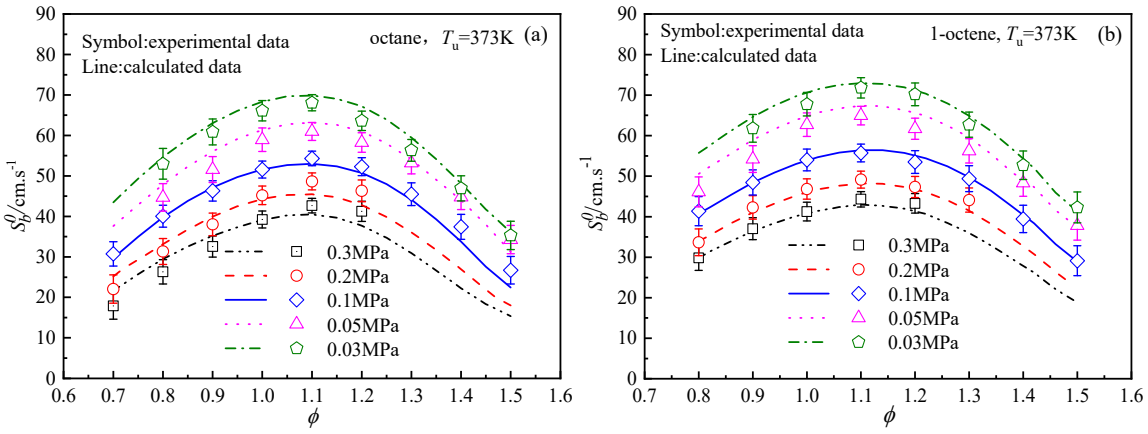

 doi:10.20944/preprints202409.2458.v1

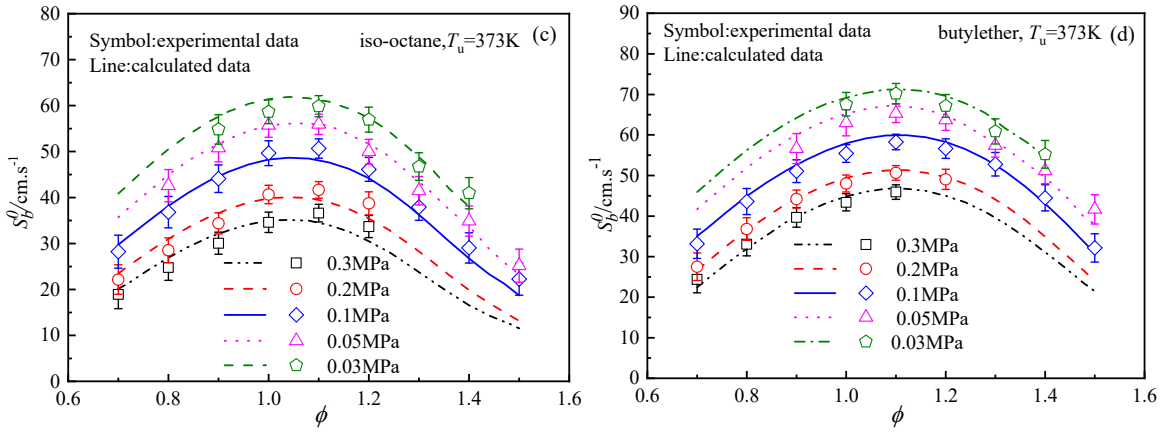

Figure 3. Laminar flame speeds of the tested fuels at Tu = 373 K for different initial pressures: (a) octane, (b) 1-octene, (c) iso-octane, (d) butylether.

Figure 4 shows the variation of laminar flame speed with initial temperature for the four tested fuels at atmospheric pressure. The laminar flame speeds of all four fuels increased as the initial temperature rises. The adiabatic flame temperature (T_{ad}), which is proportional to the laminar flame speed, can be determined from the initial temperature by the following equation:

$$T_{ad} = T_u + \frac{q_m}{C_p} Y_u \tag{11}$$

where T_u is the initial temperature of the unburned mixture, q_m is the heat released per unit mass of fuel, Y_u is the mass fraction of fuel, and C_p is the specific heat at constant pressure. Equation (11) indicates that an increase in the initial temperature of the unburned mixture results in a higher adiabatic flame temperature, which enhances the chemical reactivity and thus the laminar flame speed.

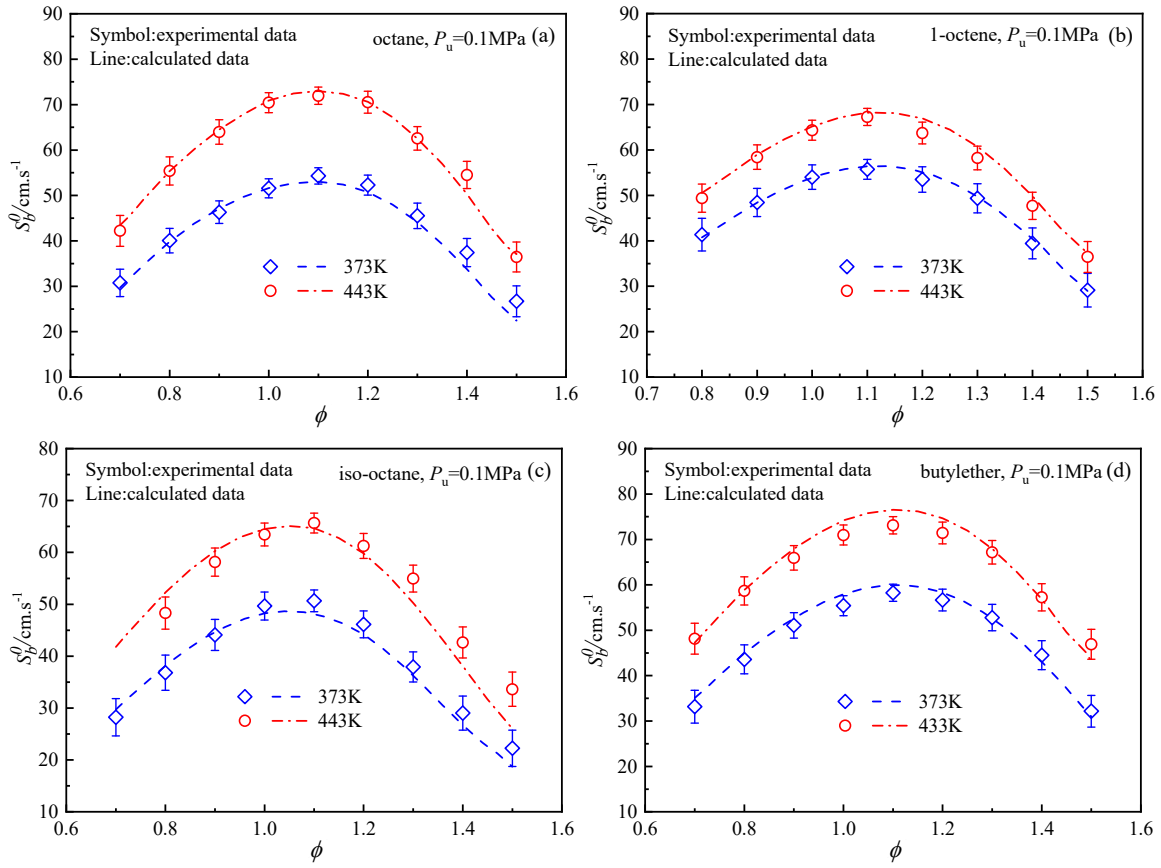

 doi:10.20944/preprints202409.2458.v1

Figure 4. Laminar flame speeds of the four test fuels at Pu = 0.1 MPa, different initial temperatures: (a) octane, (b) 1-octene, (c) iso-octane, (d) butylether.

In both Figs. 3 and 4, the lines indicate the data calculated using the kinetic mechanism obtained in Section 3 and the symbols indicate experimental data. As shown in Figure 3, at low pressures, the calculated speeds were slight overestimates compared to the experimental data, but all the differences were within the uncertainty for the laminar flame speeds. Moreover, at higher pressures for equivalence ratios up to 1.0, the experimental speeds for iso-octane and n-octane were higher than those calculated by the present model. At high pressures and high equivalent ratios, the flame was more unstable resulting in acceleration of the flame, which was responsible for this deviation. However, the numerical calculations agree well with the experimental data at atmospheric pressure, as shown in Figure 4. In summary, the kinetic mechanism described in Section 3 can predict the experimental data obtained in this research.

4.4. Analysis of the Differences in the Laminar Flame Speeds of the Four Fuels

4.4.1. Effects of Thermodynamics on the Differences in the Laminar Flame Speeds

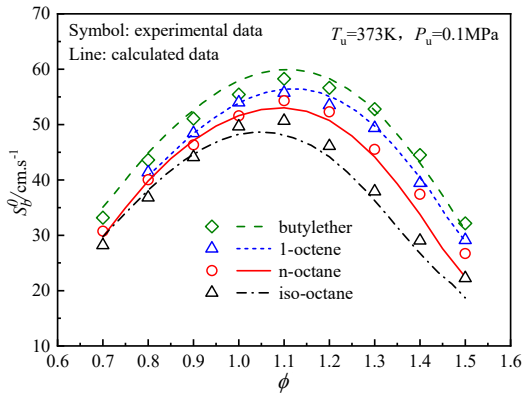

Figure 5. Comparison of laminar flame speeds for the four test fuels at Pu = 0.1 MPa, Tu = 373 K.

Figure 5 compares the laminar flame speeds of n-octane, iso-octane, 1-octene, and butyl ether at Pu = 0.1 MPa and Tu = 373 K. Butyl ether had the fastest laminar flame speed, followed by 1-octene, n-octane, and finally, iso-octane. Three factors influence the laminar flame speed: thermodynamics, diffusion, and chemical reaction kinetics[25,27]. It is necessary to determine which of these factors dominates. Based on the assumption of a one-step reaction, an equation relating the mass flow rate to the thermodynamic, transport, and chemical kinetic factors can be expressed as follows[28]:

$$\left(\rho_u S_u^0\right)^2 \sim \frac{\lambda}{C_p} Le\left[\exp\left(-\frac{E_a}{2R_0 T_{ad}}\right)\right] \quad (12)$$

where *Le* is the Lewis number and λ is the thermal conductivity. The magnitude of the thermodynamics can be characterized by the adiabatic flame temperature. Figure 6 compares the adiabatic flame temperatures of the four test fuels. In descending order, the adiabatic flame temperatures are butyl ether, 1-octene, n-octane, and iso-octane. The order of laminar flame speeds for the fuels tested exactly coincides with the relative magnitudes of their adiabatic flame temperatures, suggesting that the differences in laminar flame speeds arose in part from thermodynamic influences.

 doi:10.20944/preprints202409.2458.v1

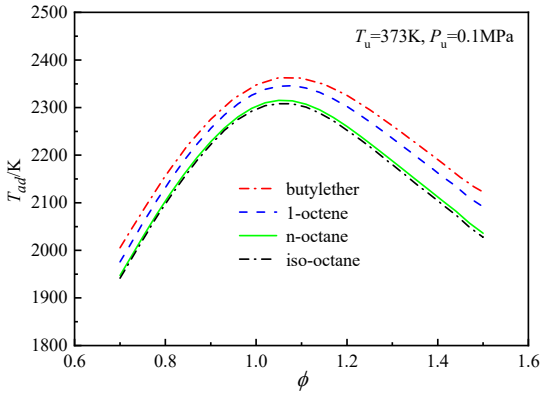

Figure 6. Comparison of adiabatic flame temperatures of the tested fuels at T = 373 K and P = 0.1 MPa.

4.4.2. Effects of Diffusion on the Differences in the Laminar Flame Speeds

The Lewis number, *Le*, is a dimensionless number, calculated as the ratio of the thermal diffusivity to the mass diffusivity. The term $(\lambda/C_P)Le$ characterizes the diffusion and is referred to as the diffusion coefficient. The laminar flame speed increased with an increase in the diffusion coefficient, so there is a positive correlation. Note that the laminar flame speed is exponentially related to both the thermodynamic and chemical kinetic factors but linearly related to diffusion. Therefore, the effect of diffusion was significantly smaller than the other two factors for the same magnitude of variation.

The diffusion coefficients of the four test fuels are compared in Figure 7. The molecular masses of the four fuels are relatively close to each other, and the actual percentage of the fuel in the mixtures is small. Hence, the diffusion coefficients of the four fuels did not differ significantly. The differences in the diffusion coefficients of the four fuels were small enough to be ignored for equivalence ratios of up to 1.0. The diffusion coefficient of iso-octane was higher than those of the other three fuels at $\phi < 1.0$, but the biggest difference was only within 0.43. It can be concluded that diffusion is not the dominant reason for the difference in the laminar flame speeds of the four test fuels. For example, iso-octane has the largest diffusion coefficient but the slowest laminar flame speed. Thus, it is also necessary to analyze the chemical kinetics to explain the difference in laminar flame speeds among the four fuels.

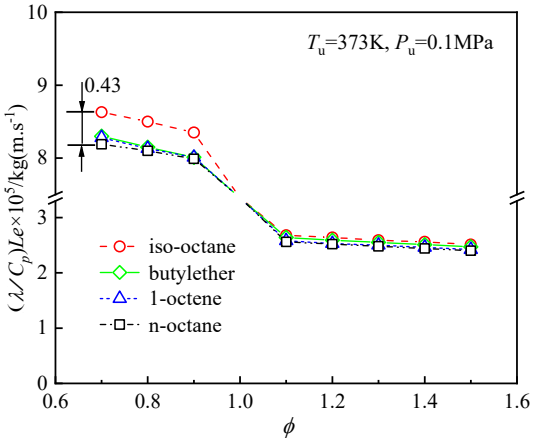

Figure 7. Diffusion effect on flames of the four tested fuels.

4.4.3. Effects of chEemical Kinetics on the Differences in the Laminar Flame Speeds

Preprints.org (www.preprints.org) | NOT PEER-REVIEWED | Posted: 1 October 2024 doi:10.20944/preprints202409.2458.v1

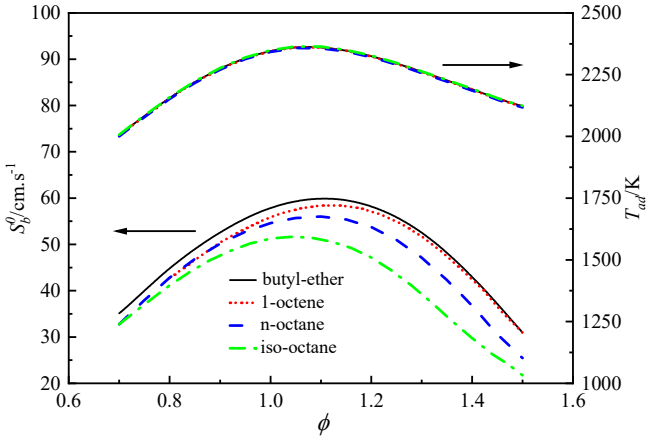

Figure 8. Laminar flame speeds under the same adiabatic flame temperatures of the four test fuels.

To separate the effects of the thermodynamics from the effects of the chemical kinetics, the laminar flame speeds of the four test fuels at the same adiabatic flame temperatures were calculated, as shown in Figure 8. Even though the adiabatic flame temperatures of the tested fuels were close to each other, there were still differences in their laminar flame speeds. The order of laminar flame speed from fastest to slowest was still butyl ether, 1-octene, n-octane, and iso-octane. The kinetic analysis is described below.

A sensitivity analysis was used to determine the key elementary reactions and the intermediate species in the flame for the four fuels. A one-dimensional freely propagating flame model was employed to calculate the sensitivity coefficient from the laminar mass flow rate and the rate constant of an elementary reaction:

$$S = \frac{\partial \ln S_u^0}{\partial \ln \alpha_i} = \frac{\alpha_i}{S_u^0} \frac{\partial S_u^0}{\partial \alpha_i} \tag{13}$$

where α_i is the pre-exponential factor. A higher sensitivity coefficient indicates that the elementary reaction makes a greater contribution to flame propagation.

A sensitivity analysis of the laminar flame speeds of the four fuels was performed at T_u = 373 K and P_u = 0.1 MPa, as shown in Figure 9. At an equivalence ratio of 1.0, the same three elementary reactions contributed the most to the laminar flame speed. These are all small-molecule reactions. The highest sensitivity coefficient was for reaction R1 (O_2 + H = OH + O). This reaction consumes an H atom to generate two active radicals, O and OH, which increases the number of active radicals. Therefore, it made the most significant contribution to the laminar flame speed. The other two reactions with high sensitivity coefficients were R2 (OH + CO = H + CO_2) and R32 (HCO + M = CO + H + M), both generating H atoms, which are highly reactive. For the lean equivalence ratio, these three reactions still had the highest sensitivity coefficients, which increased further for reaction R2. Note that the sensitivity coefficient of reaction R2 decreased as the equivalent ratio increased. Reaction R32 had a significant promoting effect on the laminar flame speed for all equivalence ratios.

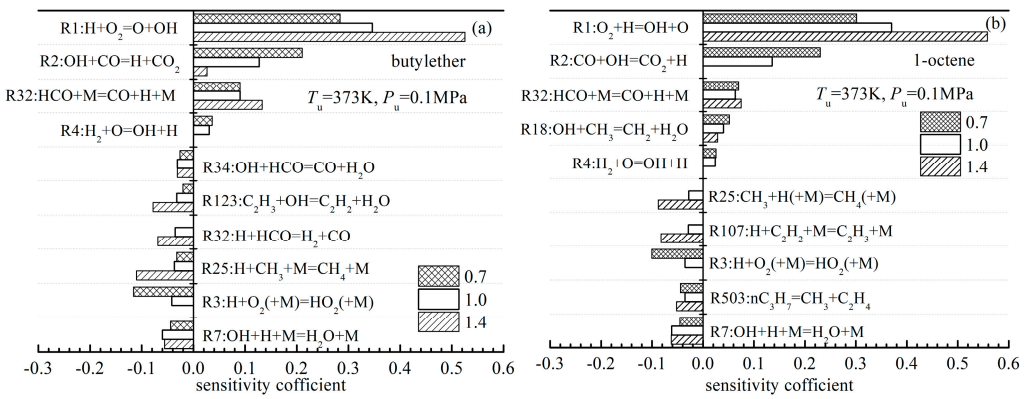

 doi:10.20944/preprints202409.2458.v1

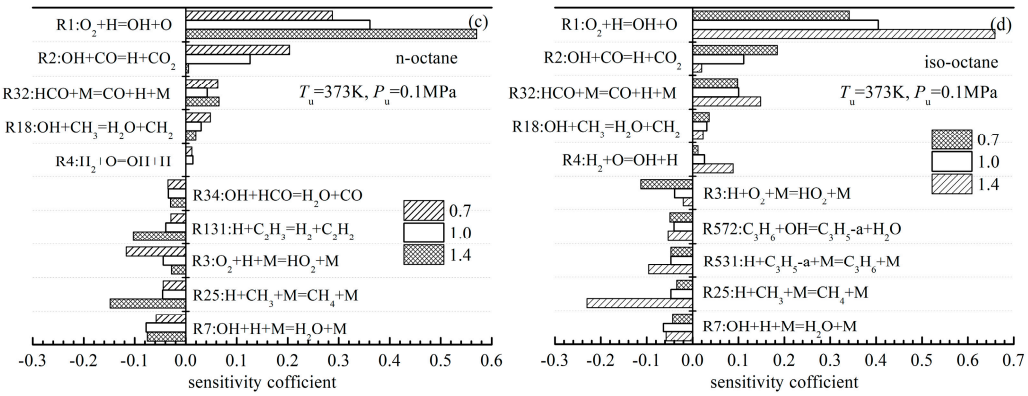

Figure 9. Sensitivity coefficient for laminar flame speeds of the four test fuels at 373 K, 0.1 MPa, and different equivalence ratios: (a) butylether, (b) 1-octene, (c) octane, (d)iso-octane .

For the four tested fuels, the reaction with the highest negative sensitivity coefficient was R7 (OH + H + M = H_2O + M). Reaction R7 consumes two highly reactive radicals OH and H to form a relatively stable radical, H_2O. It is a chain termination reaction. Another chain termination reaction, R25 (H + CH_3 = CH_4+M), consumes a highly reactive H atom to generate a stable species CH_4, which strongly inhibits the laminar flame speed. At rich equivalence ratios, the lack of oxygen in the flame led to an increase in the concentration of species CH_3, resulting in a stronger inhibition of the laminar flame speed by reaction R25 as the equivalence ratio increased. Besides, the reaction R3 (H + O_2 + M = HO_2 + M) consumes the reactive radical H, which has a significant inhibiting effect on the laminar flame speed, too. The lack of oxygen at high equivalent ratios led to a decrease in the sensitivity coefficient of reaction R3 with increasing equivalent ratio, indicating that the inhibiting effect of reaction R3 on the laminar flame speed was weaker for the rich equivalent ratio.

The differences between the laminar flame speeds of n-octane and iso-octane are obvious. In contrast, the differences in the diffusion coefficients and adiabatic flame temperatures were small. Since iso-octane has a branched chain, a large number of CH_3 radicals are produced in an iso-octane flame. The reaction R25, which consumes the radical CH_3, had a significant inhibiting effect on flame propagation. For an equivalence ratio of 1.4, reaction R5 surpassed reaction R1 as the reaction with the greatest inhibiting effect on iso-octane flame propagation. This was the main reason for the difference in laminar flame speeds between n-octane and iso-octane.

Butyl ether is the most structurally different of the four test fuels. Due to the oxygen atom on its straight chain, butyl ether has a shorter carbon chain and higher reactivity. Hence, the initial reaction of butyl ether was also very different from that of the other three fuels. The initial reaction of butyl ether was the bond-breaking reaction at the C–O bond to form n-butanol and butane. Furthermore, the generated n-butanol easily forms harmful emissions, such as aldehydes, through an H-abstraction reaction.

In summary, the sensitivity analysis was used to determine the reactions with the most significant effect on flame propagation. Furthermore, the intermediate species that strongly impacted flame propagation were determined by considering the key elementary reactions. These include H, OH, and CH_3. Among them, H and OH are active radicals and can promote flame propagation. In contrast, CH_3 is relatively stable and inhibits flame propagation.

To further clarify the differences in the chemical kinetics of the four test fuels, the concentrations of the three critical species were found by analyzing the flame structure. The concentrations of H, OH, and CH_3 at ϕ = 1.0, T_u = 373 K, and P_u = 0.1 MPa are given in Figure 10. The highest concentrations of OH and H were observed in the butylether flame, indicating that it has the highest reactivity of the four fuels. The lowest concentration of CH_3 was in the butyl ether flame. Thus, it had the weakest inhibitory effect on butylether flame propagation. These chemical kinetics are the reasons that butylether had the fastest laminar flame speed.

 doi:10.20944/preprints202409.2458.v1

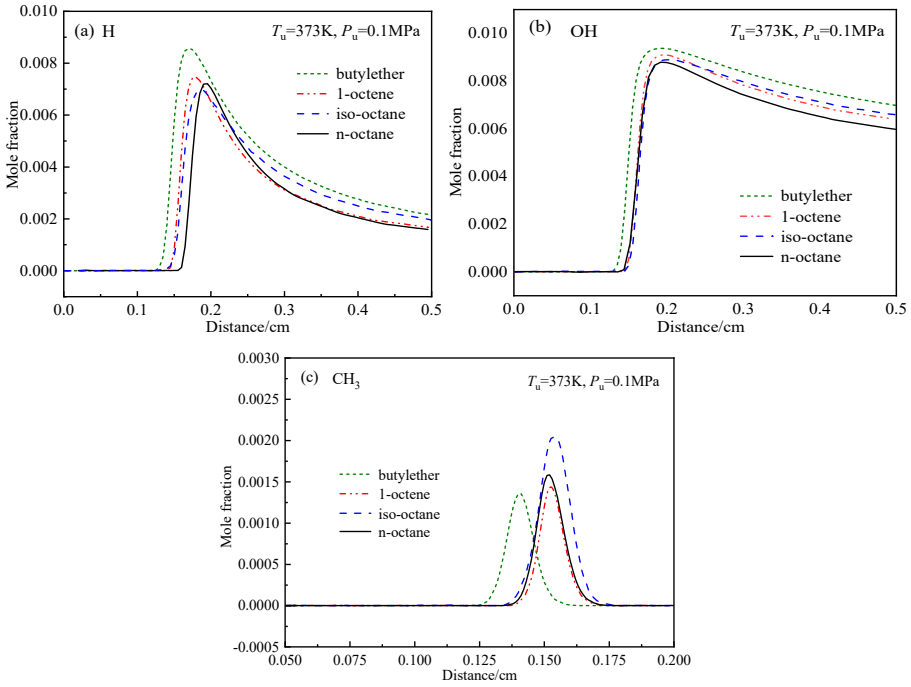

Figure 10. Concentrations of the three key species in the flames of the four fuels at T_u = 373 K, P_u = 0.1 MPa, and ϕ = 1.0 : (a) H, (b) OH and (c) CH_3.

Compared with n-octane, the higher concentrations of OH and H and lower concentrations of CH_3 can be observed in the 1-octene flame. Therefore, 1-octene has a slightly faster laminar flame speed than n-octane. Comparable concentrations of OH and H radicals are produced in the flames of iso-octane and n-octane. However, because of the branched chain on the molecular of iso-octane, the concentration of CH_3 in the iso-octane flame is remarkably higher than n-octane, indicating a stronger inhibiting effect of CH_3 on flame propagation of iso-octane. As a result, iso-octane has a slower laminar flame speed than n-octane, which is the slowest of the four tested fuels.

As well as the three key species, the concentrations of two pollutants—HCHO and ethanal (CH_3CHO)—were also calculated, as shown in Figure 11. As an oxygenated fuel, the flame of butyl ether had much higher concentrations of HCHO and CH_3CHO than the other fuels. Therefore, as an additive, butylether promotes combustion but generates higher amounts of aldehyde pollutants, which may be difficult to eliminate by post-treatment systems in practical application.

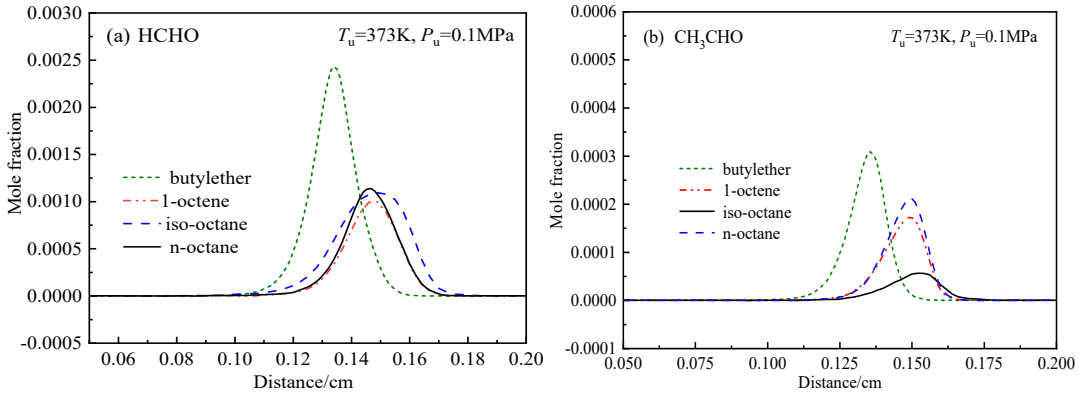

Figure 11. The concentrations of aldehyde pollutants in the flame of the four test fuels at T_u = 373 K, P_u = 0.1 MPa, and ϕ = 1.0.

5. Conclusions

 doi:10.20944/preprints202409.2458.v1

This research employed outwardly propagating spherical flames to obtain the laminar flame speeds of four C8 fuels over a wide range of initial conditions. Laminar flame speeds of four test fuels were compared. The differences in laminar flame speeds of four C8 fuels were analyzed. The main conclusions of this study are as follows:

(1)For the four test fuels, the laminar flame speeds from high to low are butylether, 1-octene, n-octane, and iso-octane.

(2)The differences in the laminar flame speeds of the four test fuels were systematically analyzed in terms of chemical kinetics, thermodynamics, and diffusion. The diffusion was small enough to be ignored. The thermodynamics had a small influence, whereas the chemical kinetics had the most significant impact on the differences in the laminar flame speeds.

(3)The different concentrations of key radicals in the flames strongly affected flame propagation. Higher concentrations of OH and H radicals, which are highly reactive, in the butyl ether flame resulted in the highest laminar flame speed. The highest concentration of the CH_3 radical was in the iso-octane flame. This radical had an inhibitory effect on flame propagation, leading to the slowest laminar flame speed.

Author Contributions: Conceptualiztion, Xin Meng and Shuai Liu; experiment implement, Shuai Liu and Ruina Li, experimental data processing, Shuai Liu and Xin Meng; numerical analysis, Jing Tian and Xin Meng; writing—original draft preparation, Xin Meng; writing—review and editing, Jing Tian and Tao Sun; funding acquisition, Ruina Li and Shuai Liu. All authors have read and agreed to the published version of the manuscript.

Funding: The research was funded by the China Postdoctoral Science Foundation Project (2019M651732), the State Key Laboratory of Automotive Safety and Energy under Project (KFY2227).

Data Availability Statement: Experimental data obtained in this study and data post-processing program can be got at "https://www.alipan.com/s/wWvZ1BKBgum".

Acknowledgments: We thank all the teachers and students in the group of professor Zhong Wang in the Jiangsu university for their guidance and help.

Conflicts of Interest: The authors declare no conflicts of interest.

References

1. Kelley A P LW, Xin Y X, et al. Laminar flame speeds, non-premixed stagnation ignition, and reduced mechanisms in the oxidation of iso-octane. Proceedings of the Combustion Institute 2011;33(1):501-8
2. Ji C SSM, Veloo P S, et al. Effects of fuel branching on the propagation of octane isomers flames. Combustion and Flame 2012;159(4):1426-36.
3. Galmiche B HF, Foucher F. Effects of high pressure, high temperature and dilution on laminar burning velocities and Markstein lengths of iso-octane/air mixtures. Combustion and Flame 2012;159(11):3286-99.
4. Broustail G HF, Seers P, et al. Experimental determination of laminar burning velocity for butanol/iso-octane and ethanol/iso-octane blends for different initial pressures. Fuel 2013;106:310-7.
5. Kelley A P SAJ, Zhu D L, et al. Laminar flame speeds of C5 to C8 n-alkanes at elevated pressures: Experimental determination, fuel similarity, and stretch sensitivity. Proceedings of the Combustion Institute 2011; 33(1):963-70.
6. Ji C DE, Wang Y L, et al. Propagation and extinction of premixed C5-C12 n-alkane flames. Combustion and Flame 2010;157(2):277-87.
7. Meng X HO, Wang T, et al. Experimental and modeling study of 1-octene jet-stirred reactor oxidation. Fuel 2017; 207:763-75.
8. Hellier P LN, Allan R, et al. The importance of double bond position and cis–trans isomersation in diesel combustion and emissions. Fuel 2013;105:477-89.
9. Cai L SA, Lee D J, et al. Chemical kinetic study of a novel lignocellulosic biofuel: Di-n-butyl ether oxidation in a laminar flow reactor and flames. Combustion and Flame 2014;161(3):798-809.
10. Guan L TC, Yang K, et al. Experimental and kinetic study on ignition delay times of di-n-butyl ether at high temperatures. Energy Fuels 2014;28(8):5489-96.
11. Wullenkord J TL-S, Böttchers J, et al. A laminar flame study on di-n-butyl ether as a potential biofuel candidate. Combustion and Flame 2018;190:36-49.
12. Kelley A P LCK. Nonlinear effects in the extraction of laminar flame speeds from expanding spherical flames. Combustion and Flame 2009;156(9):1844-51.
13. Kelley A P JG, Law C K. Critical radius for sustained propagation of spark-ignited spherical flames. Combustion and Flame 2009;156(5):1006-13.

 doi:10.20944/preprints202409.2458.v1

14. Burke MP, Chen Z, Ju YG, Dryer FL. Effect of cylindrical confinement on the determination of laminar flame speeds using outwardly propagating flames. Combustion and Flame 2009;156(4):771-9.
15. Wu C K LCK. On the determination of laminar flame speeds from stretched flames. Symposium (International) on Combustion 1985;20(1):1941-9.
16. Qiao L, Gu YX, Dam WJA, Oran ES, Faeth GM. Near-limit laminar burning velocities of microgravity premixed hydrogen flames with chemically-passive fire suppressants. Proceedings of the Combustion Institute 2007;31:2701-9.
17. Santner J HF, Ju Y, Dryer FL. Uncertainties in interpretation of high pressure spherical flame propagation rates due to thermal radiation. Combustion and Flame 2014;161:147–53.
18. Yu H HW, Santner J, Gou X, Sohn CH, Ju Y, et al. Radiation-induced uncertainty in laminar flame speed measured from propagating spherical flames. Combustion and Flame 2014;161:2815–24.
19. Moffat. Describing the uncertainties in experimental results. Exp Thermal Fluid Sci 1988;1:3–17.
20. Kee RJ GJ, Smooke MD, Miller JA, Meeks E. PREMIX: a Fortran program for modeling steady laminar one-dimensional premixed flames. Sandia National Laboratories Report 1985;SAND85-8249.
21. Kee RJ RF, Miller JA. CHEMKIN-II: a Fortran chemical kinetics package for the analysis of gas-phase chemical kinetics. Sandia National Laboratory Technical Report SAND 1989:89-8009.
22. Mehl M PWJ, Westbrook C K, et al. Kinetic modeling of gasoline surrogate components and mixtures under engine conditions. Proceedings of the Combustion Institute 2011;33(1):193-200.
23. Sarathy S M WCK, Mehl M, et al. Comprehensive chemical kinetic modeling of the oxidation of 2-methylalkanes from C7 to C20. Combustion and Flame 2011;158(12):2338-57.
24. KenjiYasunag T, Sarathy, Tohru Koikea, Fiona Gillespie, Tibor Nagy, John M.Simmie, Henry J.Curran. A shock tube and chemical kinetic modeling study of the pyrolysis and oxidation of butanols. Combustion and Flame 2012;159(6):2009-27.
25. Wu F KA, Tang C, Zhu D, Law CK. Measurement and correlation of laminar flame speeds of CO and C2 hydrocarbons with hydrogen addition at atmospheric and elevated pressures. Int J Hydrog Energy 2011;36(13171-13180).
26. Z C. On the extraction of laminar flame speed and Markstein length from outwardly propagating spherical flames. Combustion and Flame 2011;158:291-300.
27. Tang CL HZ, Law CK. Determination, correlation, and mechanistic interpretation of effects of hydrogen addition on laminar flame speeds of hydrocarbon-air mixtures. Proc Combust Inst 2011;33:921-8.
28. Law CK SC. Structure, aerodynamics, and geometry of premixed flamelets. Prog Energy Combust 2000;26:459-505.